LLNL-JRNL-463876

A Case for the Use of 3-D Attenuation Models in Ground Motion and Seismic Hazard Assessment

M. E. Pasyanos

December 9, 2010

Bulletin of the Seismological Society of America

A Case for the Use of 3-D Attenuation Models in Ground Motion and Seismic Hazard Assessment

Michael E. Pasyanos
Lawrence Livermore National Laboratory, Livermore, CA

Abstract

Attenuation relationships that are used to characterize estimated ground motion often ignore details of the earth's highly-variable three-dimensional velocity and attenuation structure. Increasingly available attenuation models can be used to refine the expected ground motions. First, some tests are performed to look at the effect of the variability in several parameters, such as crustal attenuation, upper mantle attenuation and crustal thickness. A concrete example is then provided using the results of a recent crust and upper mantle attenuation model of the Middle East. We find 30-40% variations in 1 Hz spectral accelerations simply from the variations of the same event recorded in different directions. Since overall regional variability is expected to be even higher, this effect seems significant enough to be accounted for in strong ground motion estimates and seismic hazard assessment. This has the potential to account for some of the smaller scale amplitude variations not considered using broadly applied 1-D attenuation relationships.

Introduction and Previous Work

Methods to assess seismic hazard require attenuation relationships that can estimate earthquake strong ground motions from parameters that characterize the earthquake source, the propagation path, and local site conditions. The attenuation relationships that are used to predict the ground motions from postulated events are critical to the overall quality of the assessment.

The extensive amount of work on this problem (see McGuire, 2008 for a review of the history of seismic hazard assessment) has tended to focus on regressing empirical strong ground motion data to equations of a form that tries to capture as much of the physics of the problem as possible. For example, some critical input parameters are earthquake magnitude (usually moment magnitude), some estimate of distance (epicentral distance, Joyner-Boore distance, distance to closest point on fault, etc.), site conditions (soil, soft rock, hard rock), frequency content, etc. More sophisticated analysis can also include fault type (normal, thrust, strike-slip), 3-D basin effects, sub-crustal or subduction zone earthquakes, etc. Much of this, in fact, has been the focus of Next Generation Attenuation (NGA) models and associated NGA workshops (see http://earthquake.usgs.gov/hazards/about/workshops/nga_Workshop.php and talks therein). One thing that hasn't been considered in great detail is accounting for some of the large amplitude small-scale variations in the earth's seismic attenuation.

It is, of course, quite true that there are variations in the attenuation relationships from region to region (e.g. western United States vs. eastern/central United States). There can also be some variations within a region from different authors regressing what is significantly the same strong ground motion data set (e.g. PEER strong ground motion database; http://peer.berkeley.edu/nga) using different parameterization, assumptions, weighting, etc. What these represent, however, are simply different estimates of the 1-D attenuation for broad regions.

For example, in the "2008 Update of the United States National Seismic Hazard Maps" (Petersen et al., 2008), three attenuation relationships (specifically Boore and Atkinson, 2008; Campbell and Bozorgnia, 2008; Chiou and Youngs, 2008) are equally weighted and used to characterize the attenuation structure of the western United States, including California, the Pacific Northwest, the Wasatch, and the Intermountain West, while other sets are used for Cascadia, the Central United States, the New Madrid Seismic Zone, and the Charleston Seismic Zone. We know, however, that there are significant variations in the attenuation structure of the western United States (Benz et al., 1997; Baqer and Mitchell, 1998), sometimes on small lateral scales, and that these variations will have an effect on the observed ground motions.

These attenuation relationships consider several things together. Inherent in them is the phase content of the ground motions which progress from only direct S (Sg) close to the source, then including Sn past the critical distance (and SmS at the critical distance) then finally to Lg at longer distances. The second major feature is the geometrical spreading, which characterizes the overall loss of energy and amplitude with distance independent of anelastic attenuation. Finally, there is the apparent seismic attenuation (generally characterized by the quality factor Q) which measures how both intrinsic and scattering contribute to the loss of energy and amplitude. What these relationships generally don't consider are lateral variations in the attenuation of the crust and upper mantle, often over very small distances, that can affect the amplitudes of the phases that most significantly contribute to the strong shaking.

Several questions are raised: How significant are the variations due to the attenuation effect compared to the large geometrical spreading effect? Also, since phases are not specifically culled out, how well does the distance term characterize the phase content of the ground motions? Can attenuation models determined using small magnitude events and weak ground motions contribute to improved determinations of ground motion parameters? We consider the overall effect of including variable crust and upper mantle attenuation for seismic hazard estimates. Can including lateral attenuation reduce some of the large variations in observed ground-motion parameters that result in large uncertainties in these parameters?

Some inspiration for this paper came from reading a comment in a study from Campbell and Bozorgnia (2003) that stated "The ground-motion relations do not include recordings from the 1999 M_W >7 earthquakes in Taiwan and Turkey because there is still no consensus among strong-motion seismologists as to why these events had such low ground motion." This, of course, refers to the 17 August İzmit (M 7.6) and 12 November Düzce (M 7.2) events in Turkey and the 21 September Chichi (M 7.6) event in Taiwan. Since Turkey represents one of the most highly attenuating regions of the Middle East, it would be interesting to see if amplitude variations due to attenuation could be one such cause.

Methodology

Calibrated attenuation models are becoming increasingly available for regions such as central Asia (Taylor et al., 2003), the western United States (Phillips and Stead, 2008), the Middle East (Pasyanos et al., 2009b), and East Asia (Ford et al., 2010). These models have been primarily driven by the need in nuclear explosion monitoring to reduce the scatter of regional phase amplitudes for earthquakes, and to better separate the relative P/S amplitudes of explosions in the process (e.g. Pasyanos and Walter, 2009). Accounting for regional amplitude variations is also critical in calibrating magnitude formulas that rely on regional phases, such as Pn and Lg.

In the methodology used for Mideast regional attenuation, the observed seismic amplitudes A from event i recorded at station j are parameterized as a function of four terms:

$$A_{ij} = S_i * G_{ij} * B_{ij} * P_j$$

where S is the source term, G is the geometrical spreading term, B is the attenuation term, and P is the site term. While details of all these terms are given in Pasyanos et al. (2009a and 2009b), it is worth noting here that we use a bi-linear form of geometrical spreading (Street et al., 1975) while many strong ground motion studies use tri-linear forms (e.g. Atkinson and Boore, 1995; 2006). In our tomographic inversions, we correct observed amplitudes for geometrical spreading and solve for lateral attenuation, along with source (seismic moment) and site terms. In Pasyanos et al. (2009b), the amplitudes of Pn, Pg, Sn, and Lg are inverted simultaneously, allowing us to develop attenuation models (Qp, Qs) of the crust and upper mantle.

Using this parameterization, we can generate the predicted phase amplitudes for an arbitrary earthquake of any given size and distance which is demonstrated for a simple model in **Figure 1**. For the sake of simplicity, we have first assumed a 1-D earth structure (layer over a half space) with uniform crustal thickness (30 km) and uniform apparent Q in the crust and in the upper mantle. For strong ground motion purposes, we will focus on the shear waves which will be the main source of shaking. At short distances, the main component of ground motion will be from the direct crustal shear wave which are shown as the green lines in **Figure 1a**. At some distance that depends on crustal thickness and crust and upper mantle velocities, the mantle shear-wave phase Sn (indicated by the blue lines) becomes geometric and contributes to the overall ground motion.

Figure 1b shows spectral accelerations at 1 Hz of shear-wave phases from a Mw 7 event at a hypocentral depth of 5 km as a function of distance. The Q of the crust (appropriate for the central U.S.) is given as $Q(f) = Q_o f^{\eta}$, where Q_o=640 and η=0.344 (Erickson et al., 2004). The Q of the upper mantle is 200. The amplitudes from the crustal paths (Sg and

Lg) are shown in green. Amplitudes from the mantle path before the critical distance are shown as a dashed line, since this energy is not reflected or refracted back to the surface. Where Sn does appear, it first appears as the Moho bounce SmS. This results in an increase in the total amplitudes (red lines) from distances of 80 to 90 km.

We find that the shape of the curves match the shape of regressed curves of many studies. We compare the results here to Figure 10 of Petersen et al. (2008), which compiles spectral acceleration attenuation relations for 9 different studies (**Figure 1c**). For the same event (Mw 7 on vertical strike-slip fault and Vs30 760 m/s site conditions for Central and Eastern U.S., 1.0 Hz spectral acceleration), we see variations in spectral acceleration of about 2.5 at all distances. For example, accelerations range from 0.2 – 0.5 g at 10 km to 0.02 – 0.05 g at 200 km. There is an offset between the curves in **Figures 1b and 1c** which is likely due to the different geometrical spreading and source (e.g. event depth, stress drop) assumptions between the two.

It is heartening to see that we can match the level and character of studies, at least in a qualitative sense. Most of the studies, for instance, predict a flattening of amplitudes where the mantle phase contributed to the overall ground motion. The interesting part, however, comes in seeing how variations in some of the parameters (e.g. crustal Q, mantle Q, crustal thickness) affect the predicted amplitudes.

For example, in **Figure 2a** we simply vary the crustal thickness ranging from values typical of oceanic crust (10 km) to values more characteristic for continental crust (20, 30, 40 km). What we find is that the critical distance changes from under 30 km for the thinnest crust out to about 120 km (for an event with the same source depth of 5 km). This has a relatively small effect on the amplitudes (about 10%). **Figure 2b** shows what happens when we vary the crustal Q. At 1 Hz, Q Lg typically varies from about 150 to more than 1200 (Benz et al. 1997; Romanowicz and Mitchell, 2007). The mantle Q is set to 300. While we see almost no effect over the first 40 km, by 100 km, there is a factor-of-two difference from this effect alone.

Figure 2c shows the ground motions when we vary the mantle Q by the same range, while keeping the crustal Q fixed (Qc = 300). The variability is smaller than those for the variable crustal Q. There is no effect at all on the ground motions at short distances where we only observe the direct crustal phase. Even after Sn starts coming in, it is still a smaller contribution to the total ground motion and the attenuation variations are less significant. Still, the point is clear. To various degrees, reasonable variations in these physical parameters can have a non-trivial affect on the predicted amplitudes. Next, we consider an example using values from a real attenuation model.

<u>Example</u>

We estimate the variability of ground motions due to the inclusion of 3-D attenuation. We make use of an attenuation model of the lithosphere in the Middle East (Pasyanos et al., 2009), which was developed from weak ground motions using the amplitudes of regional phases Pn, Pg, Sn, and Lg. Because this model covers apparent Qp and Qs of the crust and upper mantle, it can be used to estimate anelasticity for the primary local and regional phases.

In the model (**Figure 3**), we find one of the largest contrasts in Q between the northern Arabian Platform and the Eastern Anatolian Plateau (EAP). The Arabian Platform is late Proterozic age (Goodwin, 1996; Walter Mooney, personal communication; see http://earthquake.usgs.gov/research/structure/crust/age.html) overlain with recent sediments up to about 10 km or more with estimates of up to 8 km in the northern Arabian Platform (Laske and Masters, 1997). The crust is old and cold, and the attenuation is correspondingly low. In contrast, the EAP is part of the greater Turkish-Iranian Plateau, an active tectonic zone which is undergoing current uplift. The EAP is particularly unusual because recent studies find little or no lithospheric lid (Şengör et al., 2003; Gök et al., 2007) with the effect that heat flow in the crust is high and crustal Q is very low. In this region, the Arabian and Eurasian Plates are separated by the Eastern Anatolian Fault Zone (EAFZ) and the Bitlis-Zagros fold and thrust belt.

Large historical earthquakes have occurred along the North Anatolian Fault (NAF), including the 1939 Erzincan earthquake, which measured 8.2 on the Richter scale. The location of the event is shown by the green circle on the map in **Figure 3**. Here we postulate an event near the junction of the NAF and EAF, where the contrast in Q is particularly large. We consider two profiles, the first extending northeast into the EAP (O-A) and the second extending south into the Arabian Platform (O-B).

We calculate estimated ground motions along these two profiles for a postulated M7.0 event. Results are shown in **Figure 4**. While there is little difference in the estimated accelerations close in to the event where the geometrical spreading dominates, the differences become greater as crustal thickness differences become a factor, and as the accumulated attenuation term becomes more significant. By 250 km, there is a 30-40% difference in the estimated spectral acceleration.

These differences are significant enough to be accounted for, especially in light of the fact that they can be calibrated fairly easily with weak ground motions. And, while the example showed directional variations from one event location, regional variations in Q and accelerations could be even more significant. Nor is the example shown unique. We see similar contrasts in Q along other portions of the model, such as along the Zagros Mts. or between the Caucasus and more stable regions to the north. Large contrasts in both Q and crustal thickness can be expected between oceanic and continental crust at the continental shelf, with consequentially different ground motions. Furthermore, as the resolution of the attenuation models increase, we can expect the along-path variations to increase as well. It is possible that these types of differences could be responsible for the low ground motions in Turkey and Taiwan.

Discussion

While the effect of lateral attenuation on amplitudes is small compared to the large variations due to geometrical spreading, it seems to be an important enough effect to be accounted for. Another advantage of using lateral variations in attenuation as well as specifically culling out phases is that we can account for large changes associated with the critical distance where the mantle phases are turned back up to the surface.

While not tested rigorously, it appears that an attenuation models determined using small magnitude events and weak ground motions can contribute to improved determinations of strong ground motion parameters. In particular, the effect of crustal Q variations seems to be more significant than mantle Q or crustal thickness variations, although the latter is important for predicting ground motions at and around distances of the Moho bounce (e.g. Burger et al., 1987; Somerville and Yoshimura, 1990). It appears possible that including lateral attenuation may reduce some of the large variations in ground-motion parameters. Although this is only one component of the large variability, it may reduce overall uncertainties in predicted ground motions and needs to be considered in more detail. Because including this has the largest effect at long distances, it might be most important for estimating the contribution to hazard from infrequent, very large events that impact estimated ground motions over a large region.

Acknowledgments. This work was prepared under the auspices of the U.S. Department of Energy by Lawrence Livermore National Laboratory (LLNL) under contract DE-AC52-07NA27344. This is LLNL contribution LLNL-JRNL-******.

References

Atkinson, G. M. and D. M. Boore (1995). Ground-motion relations for eastern North America, Bull. Seism. Soc. Amer. 85, 17-30.

Atkinson, G. M. and D. M. Boore (2006). Earthquake ground-motion prediction equations for eastern North America, Bull. Seism. Soc. Amer. 96, 2181-2205.

Baqer, S. and B.J. Mitchell (1998). Regional variation of Lg coda Q in the continental United States and its relation to crustal structure and evolution, Pure Appl. Geophys., 153, 613-638.

Benz, H.M., A. Frankel, and D.M. Boore (1997). Regional Lg attenuation for the continental United States, Bull. Seism. Soc. Amer., 87, 606-619.

Boore, D.M., and G.M. Atkinson (2008). Ground-motion prediction equations for the average horizontal component of PGA, PGV, and 5%-damped PSA at spectral periods between 0.01 s and 10.0 s: Earthquake Spectra, 24 (1), 99-138.

Burger, R.W., P.G. Somerville, J.S. Barker, R.B. Herrmann, and D.V. Helmberger (1987). The effect of crustal structure on strong ground motion attenuation relations in eastern North America, Bull. Seism. Soc. Amer., 77, 420-439.

Campbell, K.W. and Y. Bozorgnia (2003). Updated near-source ground-motion (attenuation) relations for the horizontal and vertical components of peak ground acceleration and acceleration response spectra, Bull. Seism. Soc. Amer., 93, 314-331; DOI: 10.1785/0120020029.

Campbell, K.W., and Y. Bozorgnia (2008). Ground motion model for the geometric mean horizontal component of PGA, PGV, PGD and 5% damped linear elastic response spectra for periods ranging from 0.01 to 10.0 s: Earthquake Spectra, 24 (1), 139-171.

Chiou, B., and R. Youngs (2008). An NGA model for the average horizontal component of peak ground motion and response spectra: Earthquake Spectra, 24 (1), 173-215.

Erickson, D., D.E. McNamara and H.M. Benz (2004). Frequency-dependent Lg Q within the continental United States, Bull. Seism. Soc. Amer., 94, 1630–1643.

Ford, S.R., W.S. Phillips, W.R. Walter, M.E. Pasyanos, K. Mayeda, and D.S. Dreger (2010). Attenuation tomography of the Yellow Sea / Korean Peninsula from coda-source normalized and direct Lg amplitudes, Pure Appl. Geophys., DOI 10.1007/s00024-009-0023-2.

Gok, R., M.E. Pasyanos, and E. Zor (2007). Lithospheric structure of the continent-continent collision zone: eastern Turkey, Geophys. J. Int., 169, doi: 10.1111/j.1365-246X.2006.03288.x.

Goodwin (1996). Principles of Precambrian Geology, Academic Press, 327 pp.

Laske, G. and G. Masters (1997). A global digital map of sediment thickness, EOS Trans. AGU, 78, F483.

McGuire, R.K. (2008). Probabilistic seismic hazard analysis: Early history, Earthquake Engng Struct. Dyn. 2008; 37:329–338, DOI: 10.1002/eqe.765.

Pasyanos, M.E., and W.R. Walter (2009). Improvements to regional explosion identification using attenuation models of the lithosphere, Geophys. Res. Lett., 36, L14304, doi 10.1029/2009GL038505.

Pasyanos, M.E., E.M. Matzel, W.R. Walter, and A.J. Rodgers (2009a), Broad-band Lg attenuation modeling of the Middle East, Geophys. J. Int., 177, 1166-1176, doi:10.1111/j.1365-246X.2009.04128.x

Pasyanos, M.E., W.R. Walter, and E.M. Matzel (2009b). A simultaneous multi-phase approach to determine P-wave and S-wave attenuation of the crust and upper mantle, Bull. Seismol. Soc. Amer., 99, 3314–3325, doi 10.1785/0120090061.

Petersen, M.D., A.D. Frankel, S.C. Harmsen, C.S. Mueller, K.M. Haller, R.L. Wheeler, R.L. Wesson, Y. Zeng, O.S. Boyd, D.M. Perkins, N. Luco, E.H. Field, C.J. Wills, and K.S. Rukstales (2008). Documentation for the 2008 Update of the United

States National Seismic Hazard Maps: U.S. Geological Survey Open-File Report 2008–1128, 61 p.

Phillips, W.S., and R.J. Stead (2008). Attenuation of Lg in the western US using the USArray, Geophys. Res. Lett., 35, L07307, doi 10.1029/2007GL032926.

Romanowicz, B., and B.J. Mitchell (2007). Deep Earth structure – Q of the Earth from crust to core, in Treatise of Geophysics (ed. G. Schubert), Vol. 1, 731-774.

Şengör, A.M.C., S. Özeren, T. Genç, and E. Zor (2003). East Anatolian high plateau as a mantle-supported, north–south shortened domal structure. Geophys. Res. Lett., 30 (24), 8045, doi:10.1029/2003GL017858.

Somerville, P. and J. Yoshimura (1990). The influence of critical Moho reflections on strong ground motions recorded at San Francisco and Oakland during the 1989 Loma Prieta earthquake, Geophys. Res. Lett., 17, 1203-1206.

Street, R.L., R.B. Herrmann, and O.W. Nuttli (1975). Spectral characteristics of the Lg wave generated by central United States earthquakes, Geophys. J. R. Astr. Soc. 41, 51-63.

Taylor, S.R., X. Yang, and W.S. Phillips (2003). Bayesian Lg attenuation tomography applied to Eastern Asia, Bull. Seismol. Soc. Amer. 93, 795–803.

Figure Captions

Figure 1. a) Cartoon of raypaths from an earthquake on a vertical strike-slip fault through a 1-D structure. Raypaths that bottom in the crust are shown in green, while raypaths that bottom in the mantle are shown in blue. b) Median 1.0 s spectral acceleration (in standard gravity) as a function of distance (in km) for the crustal phase (green line), mantle phase (blue line), and total (red line). The mantle phase is dashed where it is an non-geometric arrival. c) Spectral acceleration (SA) attenuation relations from nine studies for the central and eastern United States (Figure 10 from Petersen et al., 2008).

Figure 2. Estimated ground motions (1 Hz spectral acceleration) for a postulated Mw 6.5/7.0 event for a number of earth models. a) Qc = 300, Qm = 300, crustal thickness = 10, 20, 30, 40 km. b) crustal thickness = 30 km, Qm = 300, Qc = 150, 300, 600, 1200. c) crustal thickness = 30 km, Qc = 300, Qm = 150, 300, 600, 1200.

Figure 3. Map of eastern Turkey and surrounding regions showing crustal Qs. Plate boundaries are indicated by the thick black lines and cross-sections by the thick gray lines. Green circle is the location of the 1939 Erzincan earthquake, while yellow circle shows the theoretical earthquake location. NAF = North Anatolian Fault, EAF = East Anatolian Fault, EAP = Eastern Anatolian Plateau, DSF = Dead Sea Fault. Figures to the right show Q along profiles indicated on the map.

Figure 4. Estimated ground motions (1 Hz spectral acceleration) for a postulated $M_w7.0$ event along two profiles indicated in the previous figure. Source and site terms are fixed along the two profiles.

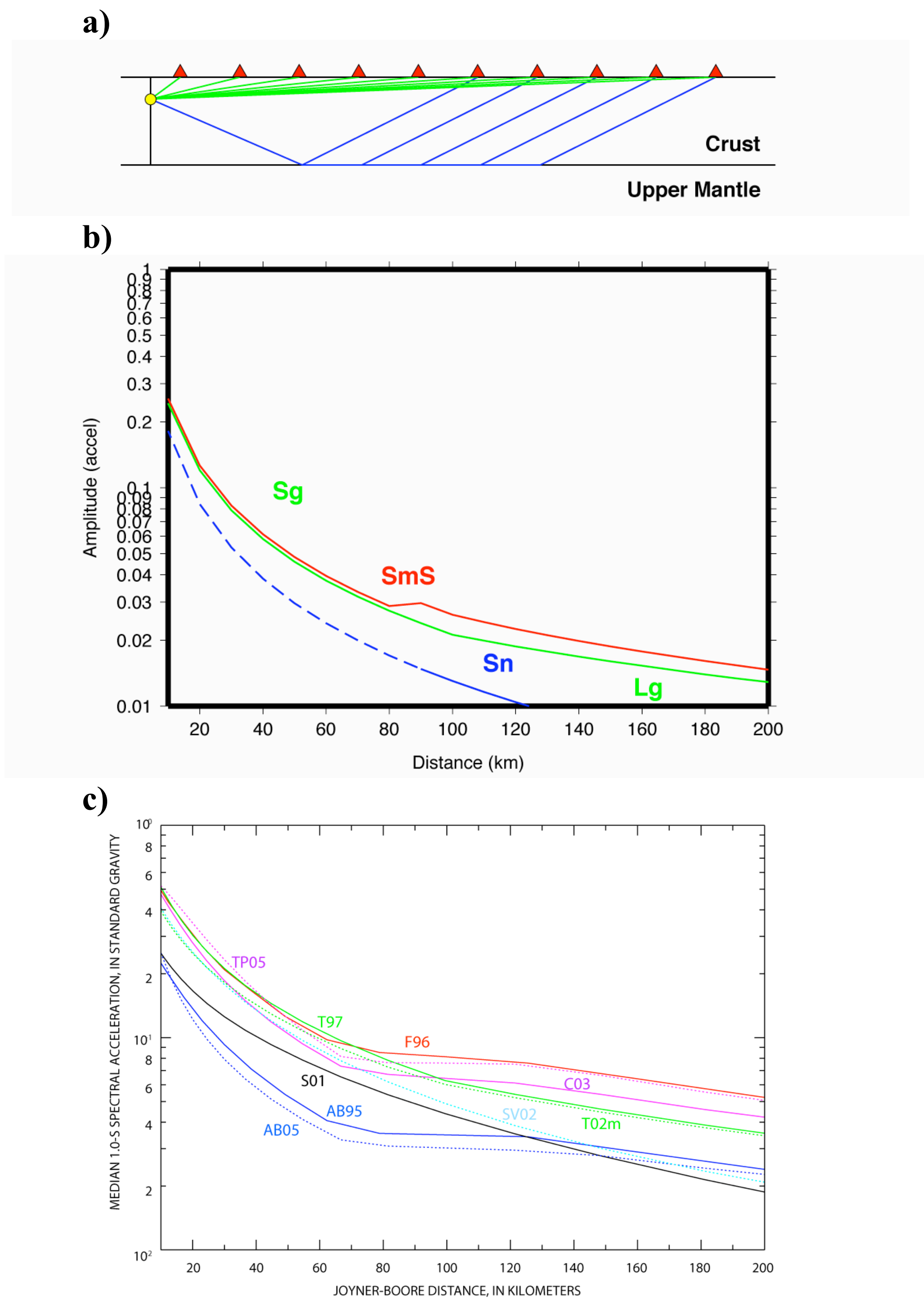
a)
Crust
Upper Mantle
b)
Amplitude (accel)
Sg
SmS
Sn
Lg
Distance (km)
c)
MEDIAN 1.0-S SPECTRAL ACCELERATION, IN STANDARD GRAVITY
TP05
T97
F96
S01
C03
AB95
AB05
SV02
T02m
JOYNER-BOORE DISTANCE, IN KILOMETERS

Figure 1.

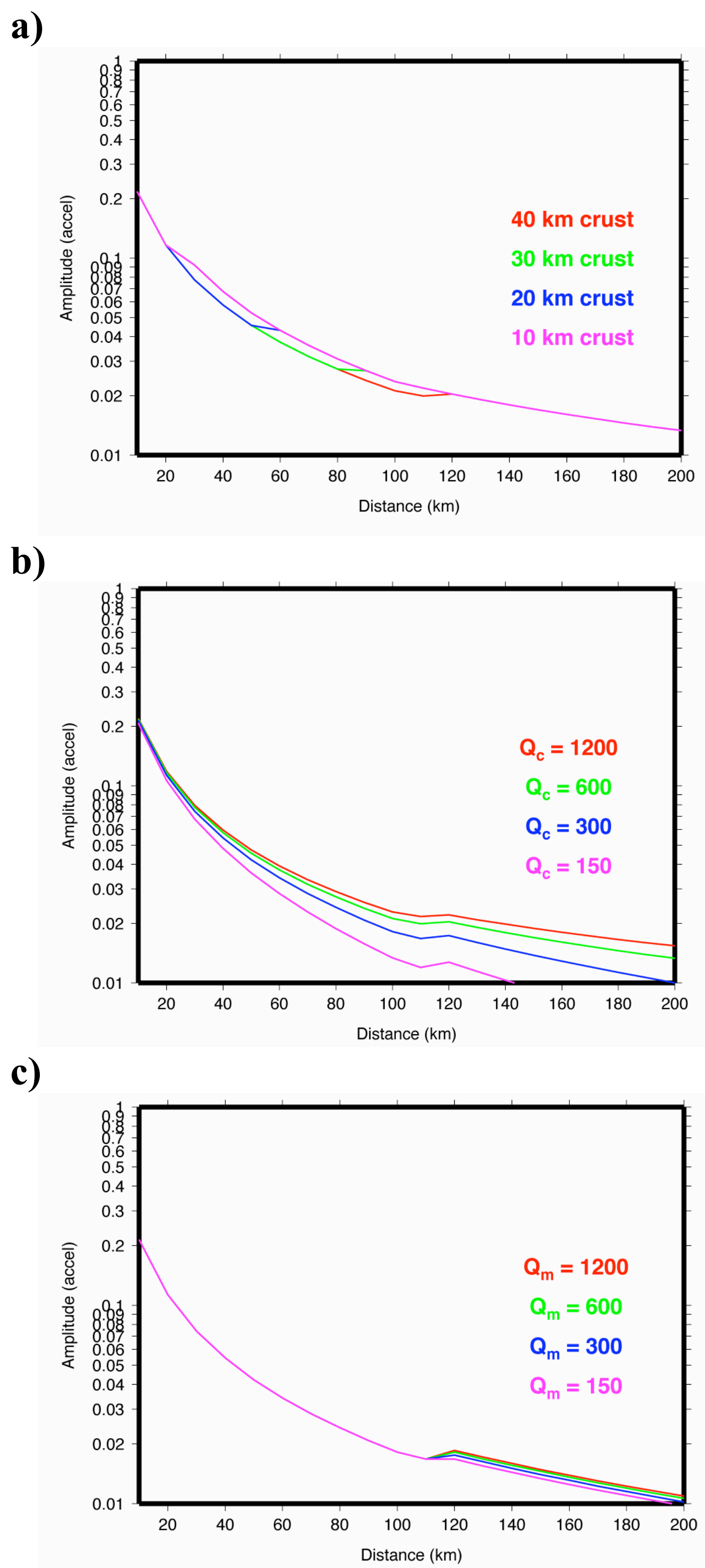
a)
Amplitude (accel)
Distance (km)
40 km crust
30 km crust
20 km crust
10 km crust
b)
Amplitude (accel)
Distance (km)
Q_c = 1200
Q_c = 600
Q_c = 300
Q_c = 150
c)
Amplitude (accel)
Distance (km)
Q_m = 1200
Q_m = 600
Q_m = 300
Q_m = 150

Figure 2.

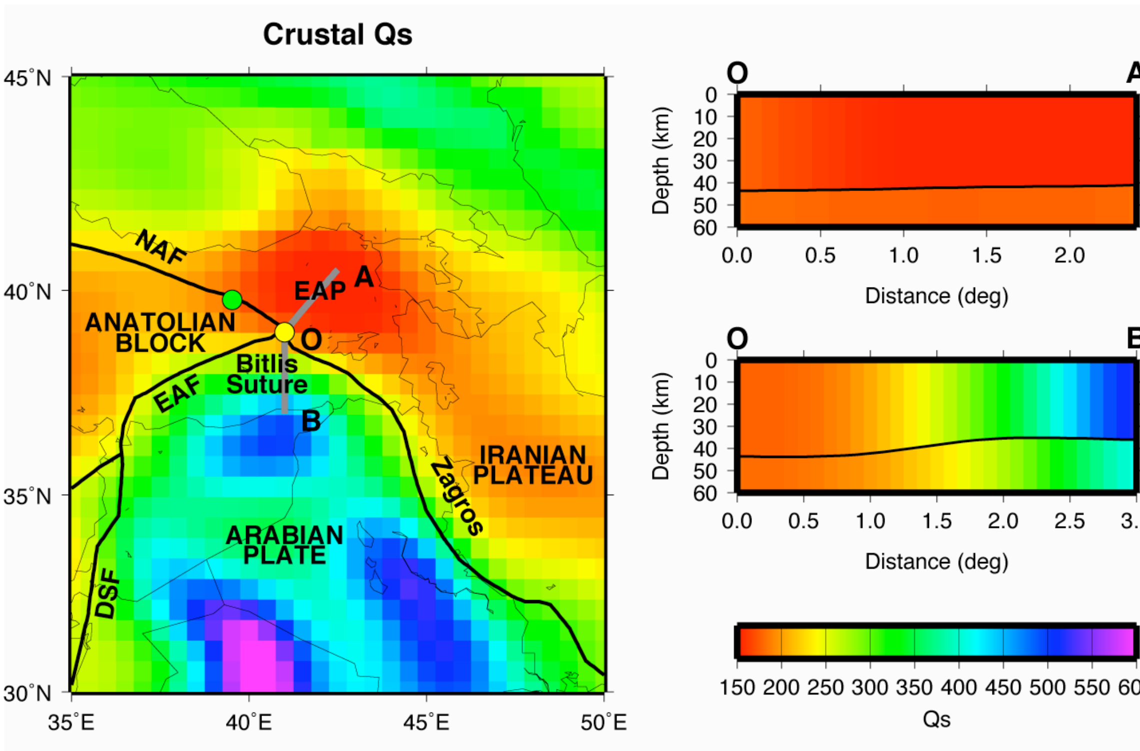

Crustal Qs
45˚N
40˚N
35˚N
30˚N
35˚E
40˚E
45˚E
50˚E
NAF
EAP
A
ANATOLIAN
BLOCK
O
Bitlis
Suture
EAF
B
IRANIAN
PLATEAU
Zagros
ARABIAN
PLATE
DSF
O
A
Depth (km)
Distance (deg)
O
B
Depth (km)
Distance (deg)
150 200 250 300 350 400 450 500 550 600
Qs

Figure 3.

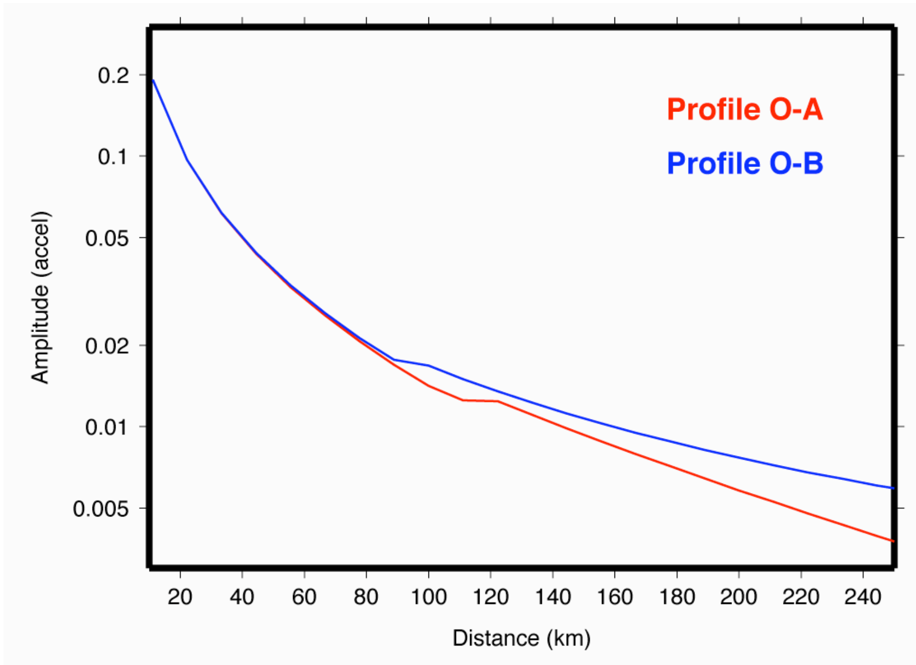

Profile O-A
Profile O-B
Amplitude (accel)
0.2
0.1
0.05
0.02
0.01
0.005
20
40
60
80
100
120
140
160
180
200
220
240
Distance (km)

Figure 4.